Software Implementation of Higher-Order Elements

VIERA BIOLKOVÁ[1)], DALIBOR BIOLEK[2,3)], ZDENĚK KOLKA[1)]
Departments of Radioelectronics [1)] and Microelectronics [2)], Brno University of Technology
Department of Electrical Engineering [3)], University of Defence Brno
CZECH REPUBLIC
dalibor.biolek@unob.cz http://user.unob.cz/biolek

Abstract: - The idea of mutual transformations between the neighbouring elements in Chua's periodical table of fundamental higher-order elements is described. These transformations are provided via four mutators, each of them being implemented via two methods. Behavioral models of these eight mutators can be used for experimenting in SPICE-compatible simulation programs, when the behavior of an arbitrary higher-order element from Chua's table can be simulated only on the basis of the knowledge of its constitutive relation.

Key-Words: -Mutator, constitutive relation, higher-order element, Chua's periodical table.

1 Introduction

The fabrication of the so-called HP memristor in the Hewlett-Packard laboratories in 2008 [1], i.e. a nanodevice which exhibits the memristor behavior [2], initiated a growing interest of experts in circuit elements such as memristor, memcapacitor, and meminductor [3], particularly as a consequence of the visions of their utilization in computer memories [4] and in artificial intelligence systems [5]. An analysis of L. Chua's theoretical articles from the eighties of 20th century points to the fact that memristor, memcapacitor, and meminductor belong to the general system of the so-called higher-order elements (HOEs) or (α,β) elements [6], arranged in a two-dimensional table. Each element is addressed in this table by two indices (α,β), where α represents the order of time-domain differentiation (if $\alpha > 0$) or integration (if $\alpha < 0$) of the terminal voltage of the element, with general notation $v^{(\alpha)}$. Accordingly, β represents the order of time-domain differentiation or integration of the current flowing through the element, with general notation $i^{(\beta)}$. The (α,β) element is then defined axiomatically by the generally nonlinear constitutive relation (CR) between the $v^{(\alpha)}$ and $i^{(\beta)}$ variables. The CR characterizes only this element and it does not depend on its neighbourhood. It is shown in [6] that the HOEs form a set of fundamental elements for modeling complicated phenomena, for example also in the world of nanotechnologies.

Conventional circuit elements such as resistor (R), capacitor (C), and inductor (L) are HOEs with the indices (0,0), (0,-1), and (-1, 0), and the indices of their memory versions, i.e. memristor (RM), memcapacitor (MC), and meminductor (ML) are (-1,-1), (-1,-1), and (-2,-1). Little information has been published about the other HOEs [7], [8].

Currently, a lot of computer models of memristors, memcapacitors, and meminductors exists which are based on the techniques of physical modeling [9]-[13] and behavioral modeling, the latter starting particularly from the CRs of these elements [14]-[16]. For modeling the element behavior on the basis of their CR, it is advantageous to use classical mutators [17], which transform the nonlinear CR of a concrete element into a shape-similar CR of another element from Chua's table. In this way, we can implement, for example, the memcapacitor from the memristor and mutator for memristor-memcapacitor transformation [18], [19]. These techniques were built already during the eighties of 20th century by introducing mutators for mutual transformation of HOEs [8]. As an advantage of this approach, the simulated HOE has a correctly defined CR, thus it behaves as an ideal element. This is not the case of several currently used modeling techniques. For example, the memcapacitor and meminductor are modeled in [20] by means of simple transforming circuits and the memristor. However, such a transformation does not retain the CR. As a consequence, the elements modeled do not show all the fingerprints of memcapacitors and meminductors.

In the case of the necessity of the analysis of a concrete HOE, it is not reasonable to use a model which does not embody all the fingerprints of this element. It is useful if the model starts from the CR, which includes all the characteristics of the HOE. This approach can be combined with the mutator technique. For example, we can start with the nonlinear current-voltage characteristic of the resistor which is transformed via the corresponding mutator into the CR of an arbitrary HOE. This element is then simulated between the mutator terminals.

ISBN: 978-1-61804-108-1

The above procedure is used in the paper for modeling arbitrary HOEs via SPICE-compatible simulation programs. The following Section shows the procedure of building the models of mutators for transforming the HOE in Chua's table into an arbitrary element in its nearest neighbourhood. A possible implementation of these models in the simulation program is explained in Section 3. Section 4 shows one way of working with the mutator models when modeling selected HOEs.

2 Mutators for transforming neighbouring elements in Chua's table

Consider an arbitrary HOE in Chua's table in Fig. 1 (a), for example the (0,0) element, i.e. resistor. It has eight neighbours. The nearby elements (0,1) and (0,-1) are accessible via "vertical transformations", which can be denoted by the symbols ↑↓. The elements (-1,0) and (1,0) can be touched via "horizontal transformations" of the type of ←→. The remaining elements (1,1), (-1,-1), and (-1,1), (1,-1) are obtained via "diagonal transformations" of the type of ↗↙ and ↖↘.

Now consider a general (α,β) HOE with a CR

$$f(v^{(\alpha)}, i^{(\beta)}) = 0 \qquad (1)$$

where f is a nonlinear function of higher-order differentiations or integrals of element voltage and current. Let us limit the modeling to such a HOE whose CR (1) can be derived as a single-valued functional dependence of $i^{(\beta)}$ on $v^{(\alpha)}$ (the so-called voltage-controlled element) and also as a single-valued functional dependence of $v^{(\alpha)}$ on $i^{(\beta)}$ (the so-called current-controlled element). Then the graphs of both dependences will be monotonic. An example of the graph of such a CR of voltage-controlled (α,β) element is in Fig. 2 on the left. The indices 1, 2 denote voltages and currents of the original and transformed elements. The purpose is to find a mutator which would transform a given element into some neighbouring (α+a,β+b) element, where a, b are numbers from the set {-1,0,1}. This transformation must preserve the shape of the CR of the original element. This requirement is marked in Fig. 2 by physical coefficients k_x and k_y which appear in the equations for the axis transformation.

Utilizing the identities

$$v_2^{(\alpha+a)} = k_x v_1^{(\alpha)} \Rightarrow v_2^{(a)} = k_x v_1^{(0)} = k_x v_1 \Rightarrow v_2 = k_x v_1^{(-a)},$$

the axis transformation can be expressed as follows:

$$v_2 = k_x v_1^{(-a)},\ i_1 = \frac{1}{k_y} i_2^{(b)}, \qquad (2)$$

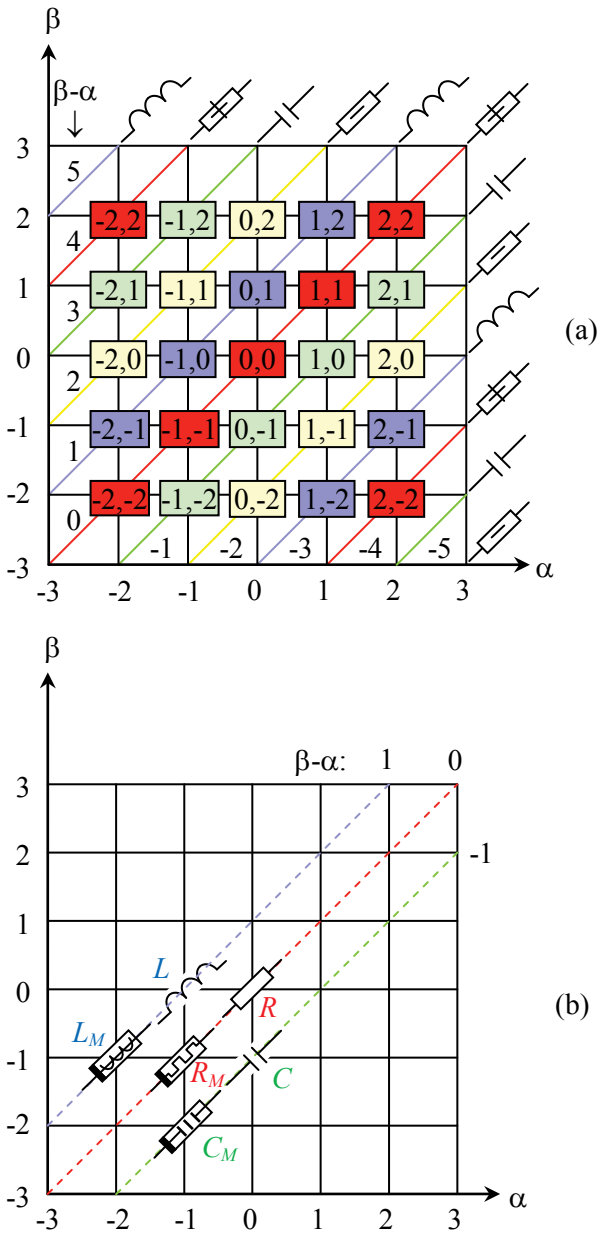

Fig. 1: (a) Chua's periodical table of (α, β) elements. Adopted from [6] and modified. Each box with α, β numbers denotes (α, β) element. (b) The location of resistor (R), capacitor (C), inductor (L), memristor (RM), memcapacitor (CM), and meminductor (LM) in the table.

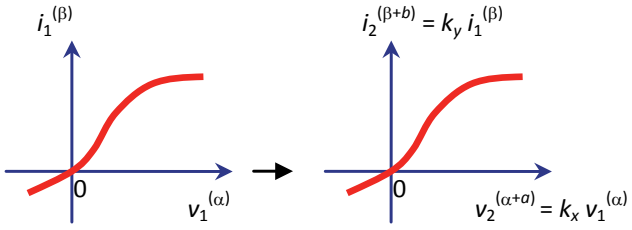

Fig. 2: Transformation of (α,β) element into (α+a,β+b) element.

ISBN: 978-1-61804-108-1

or

$$v_1 = \frac{1}{k_x} v_2^{(a)}, \; i_2 = k_y i_1^{(-b)}. \tag{3}$$

Note that the coefficients k_x and k_y have their concrete significance for the conversion between the differential parameters of the original and transformed elements:

$$\frac{di_2^{(\beta+b)}}{dv_2^{(\alpha+a)}} = \frac{k_y}{k_x} \frac{di_1^{(\beta)}}{dv_1^{(\alpha)}}. \tag{4}$$

Equations (2) and (3) can be understood as mathematical models of the mutators in Fig. 3.

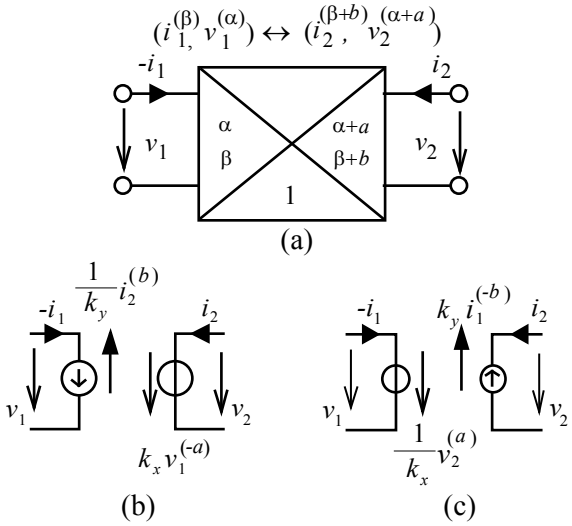

Fig. 3: (a) schematic symbol of the mutator according to [2], (b) realization 1 (I,V), (c) realization 2 (V,I).

Realization 1 utilizes Eq. (2) for modeling port 1 via controlled current source and for modeling port 2 via controlled voltage source (hence the notation (I,V)). Equation (3) then leads to realization 2 of the (V,I) type. The negative sign of the current i_1 is chosen with respect to the sink orientation of voltage and current of port No. 1 for connecting the (α,β) element.

Note from Figs 3 (b), (c) that the variables of the controlled sources are given by higher-order integrals or differentiations of circuit variables, with orders given by the numbers a and b, which depend on the distance between the original and the transformed element in Chua's table. This order is not higher than 1 for the neighbouring elements. This can be advantageous also from the point of view of the numerical solution of the model in a simulation program. It is also obvious that the mutator model does not depend on the indices of the original element, and thus it can be used uniformly - for example for resistor-inductor transformation or also for capacitor-memristor transformation. The transformation between arbitrary two elements can be implemented subsequently via a cascade connection of the corresponding mutators. It is necessary to avoid the potential conflicts in the connection of the sources of the same type. This can be accomplished by a proper connection of the ports of the realizations (I,V) and (V,I).

For computer modeling of HOEs, the universal mutators are for a = 0, 1, -1, and b = 0, 1, -1. Such mutators can serve for the transformation of the elements in the table with incremental shifts to the right →or to the left ← (a=1 or -1, b = 0), up ↑ or down ↓ (a = 0, b = 1 or -1), cornerwise in ↗ or ↙ direction (a = 1, b = 1, or a = -1, b = -1), or cornerwise in ↖ or ↘ direction (a = -1, b = 1, or a = 1, b = -1).

Note that the mutator for transforming the (α,β) element from port 1 into the (α+a,β+b) element emulated at port 2 exhibits symmetrical behavior such that after connecting the (α+a,β+b) element to port 2, it will be transformed into the (α,β) element at port 1. Then, for example, a mutator for → transformation can be used also for the reverse ← transformation.

3 Model implementation in the simulation program

The models of eight mutators (4 for (I,V) and 4 for (V,I) realizations) for the above four incremental transformations were implemented in the Micro-Cap program [21]. Since it is a SPICE-compatible program, this procedure can be used for similar implementation in the well-known PSpice or other programs.

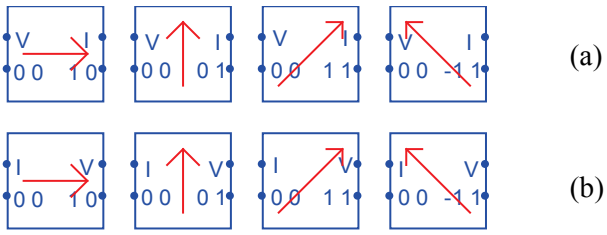

Fig. 4: Schematic symbols of implemented mutators, (a) realization (V,I), (b) realization (I,V).

The schematic symbols are shown in Fig. 4. Each port is denoted by a V or I symbol according to the type of the source connected to the port. It prevents

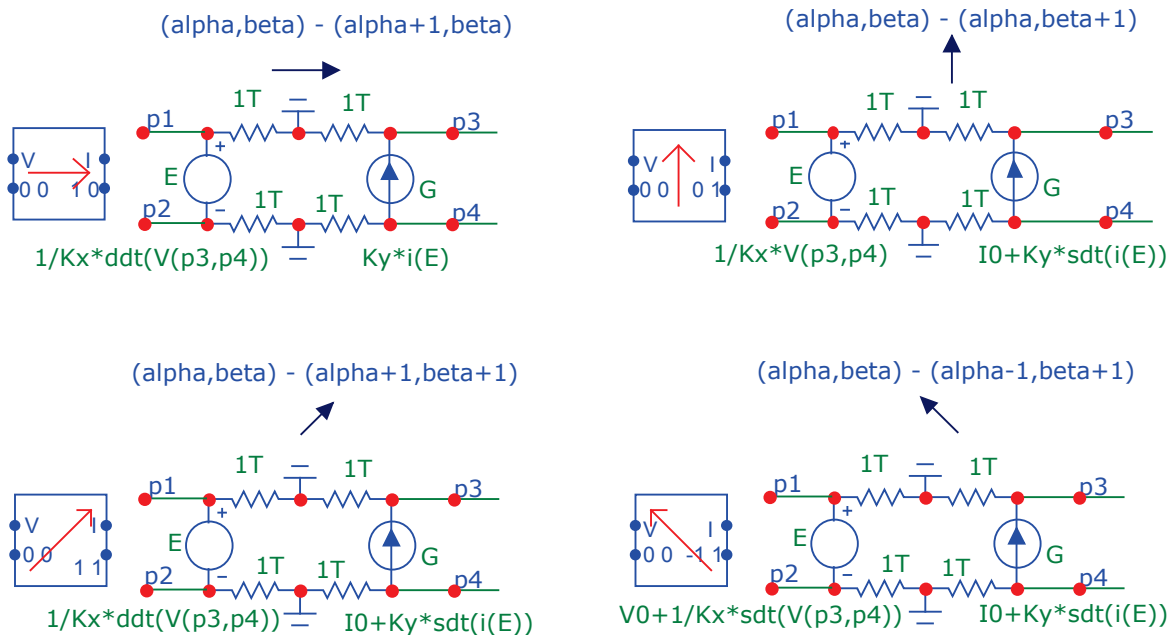

Fig. 5: Implementation of mutators of realization (V,I) in Micro-Cap.

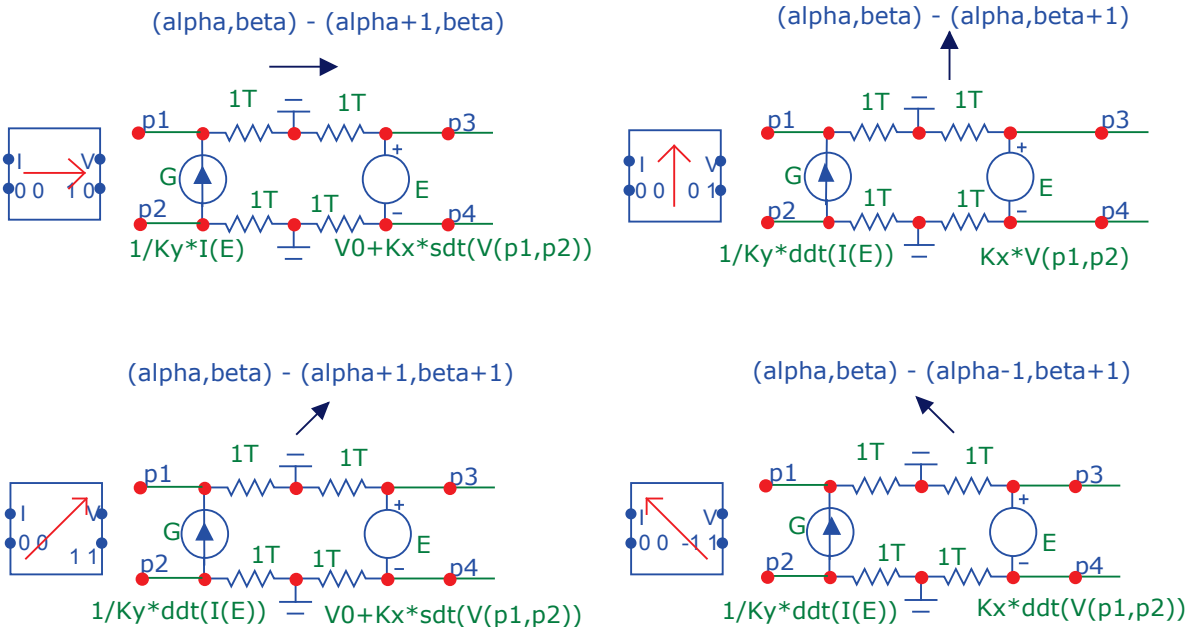

Fig. 6: Implementation of mutators of realization (I,V) in Micro-Cap.

the potential conflicts of the same sources being connected together. The direction of the transformation in Chua's table is symbolized by an arrow and also by the indices α and β near the individual ports (in the sense of their increments).

Figures 5 and 6 summarize the behavioral models of all mutators employing controlled sources. The *ddt* and *sdt* are standard PSpice functions for time-domain differentiation and integration. These operations can be implemented via various well-known methods in concrete simulation programs, or they can be modified in order to eliminate potential convergence problems in the simulation of numerically exacting tasks. The transformation coefficients k_x, k_y and the initial conditions V_0, I_0 can be defined by the user during the call of the mutator macro.

4 Demonstration of HOE modeling

A demonstration of memristor modeling via the transformation of nonlinear resistor by the ↗↙-type mutator is shown in Fig. 7. The resistor is modeled

ISBN: 978-1-61804-108-1

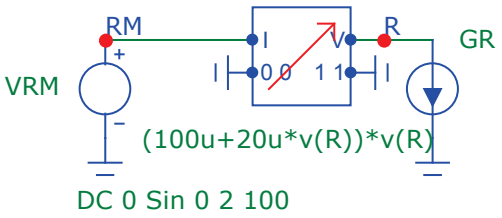

Fig. 7: An example of memristor implementation via a nonlinear resistor, modeled by controlled current source, and (I, V) ↗↙ mutator.

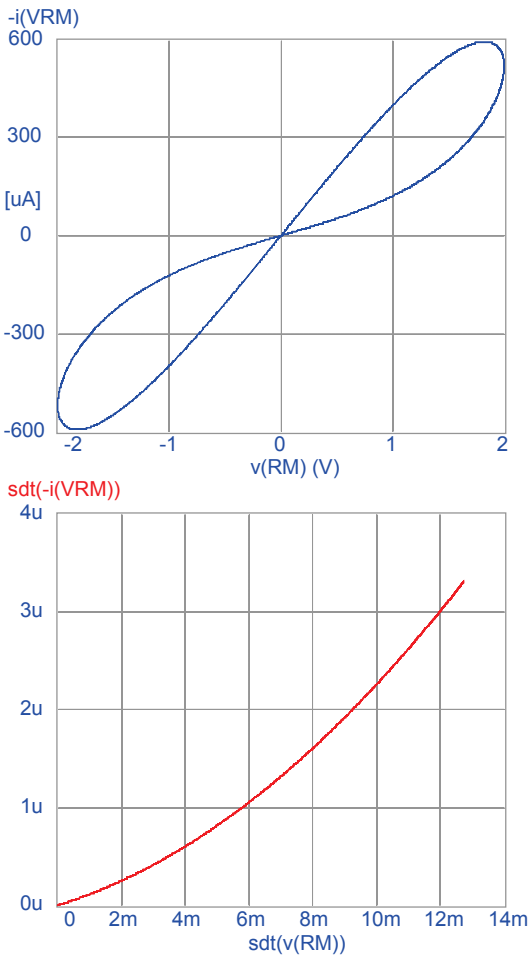

Fig. 8: Results of Transient analysis of the memristor from Fig. 7: hysteretic current-voltage characteristic and charge-flux CR.

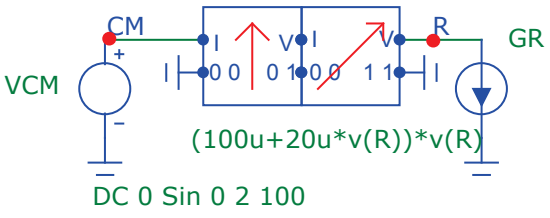

Fig. 9: An example of memcapacitor implementation via a nonlinear resistor and a cascade of two (I, V) ↗↙ and ↑↓ mutators.

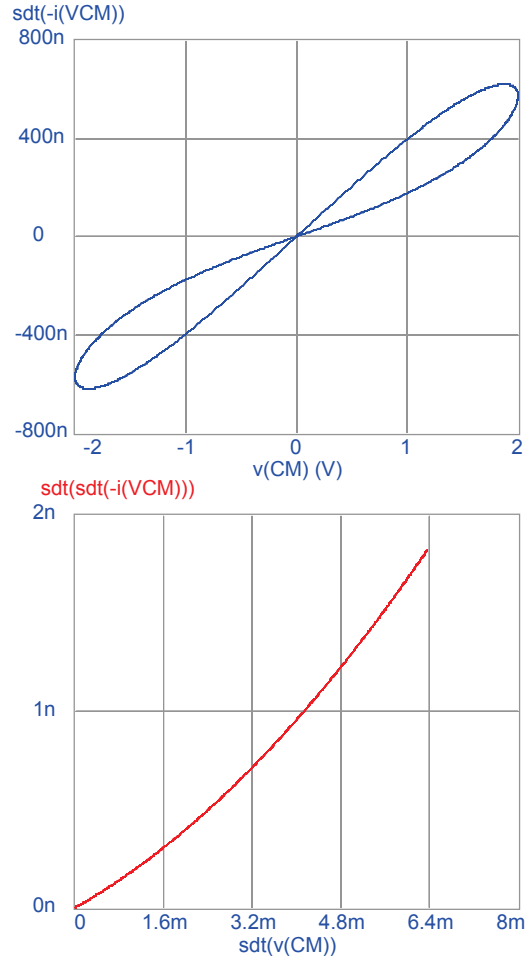

Fig. 10: Results of Transient analysis of the memcapacitor from Fig. 9: hysteretic coulomb-voltage characteristic and charge integral-flux CR.

via a controlled current source. It results from the mathematical description of the controlled source that the conductance is 100μS (and the resistance is 10 kΩ) for a low voltage on the simulated resistor, and that this conductance increases with increasing voltage.

The mutator is excited on the memristive port (RM) by a sinusoidal voltage source with an amplitude of 2V, frequency of 100 Hz, and zero initial phase (the signal is described by the "sin" function). As can be seen from the mutator model in Fig. 6, this voltage is transformed into the resistive port "R" via time-domain integration and multiplication by a coefficient k_x. For the frequency of 100 Hz, the transformation is done with the ratio of amplitudes $k_x/(2\pi.100)$. For k_x = 628, the voltage swing on the resistive and memristive ports will be the same on the frequency of 100 Hz. Then the nonlinear resistor will be excited with large dynamics, which accomplishes the nonlinear

ISBN: 978-1-61804-108-1

phenomena necessary for the hysteretic effects on the memristive port. For higher frequencies, the voltage swing on the resistive port will go down, which causes the well-known fading of the hysteresis in the current-voltage characteristic on the memristive port. The coefficient k_y has been designed the same as k_x. Then the resistor with the differential resistance R will be transformed into a memristor with the memristance $R_M = R$ (see Eq. 4). Figure 8 shows a typical pinched hysteretic loop of the memristor and its charge-flux CR, the latter copying the shape of the current-voltage characteristic of the resistor. The Transient analysis confirms the well-known collapse of the hysteresis effects at higher frequencies, and also the CR independence of the type of the excitation signal.

The circuit in Fig. 9 extends the configuration from Fig. 7 by a mutator of the ↑↓ type. The memristor is thus transformed into a memcapacitor (see also Fig. 1). The coefficients k_x=1 and k_y=628 of the mutator provide identical impedances at both its ports for the frequency of 100 Hz. On the assumption of linear operation, connecting a linear resistor of 10 kΩ resistance at the "R" port results in a capacitor without memory effect with a capacitance of 159 nF, simulated at port "CM".

Acknowledgments

This work has been supported by the Czech Science Foundation under grant No P102/10/1614, by the Project for the development of K217 Department, UD Brno – Modern electrical elements and systems, and by projects SIX and WICOMT, CZ.1.05/2.1.00/03.0072 and 1.07/2.3.00/20.0007.

References:

[1] Strukov, D. B. et al. The missing memristor found. *Nature*, 1 May 2008, pp. 80-83.

[2] Chua, L. O. Memristor–the missing circuit element. *IEEE Trans. Circ. Theory*, vol. CT-18, no. 5, 1971.

[3] Di Ventra, M., Pershin, Y.V., Chua, L.O. Circuit elements with memory: memristors, memcapacitors and meminductors. *Proceedings of the IEEE*, vol. 97, no.10, 2009, pp. 1717-1724.

[4] Chua, L. O. Resistance switching memories are memristors. *Applied Physics A, Materials Science & Processing*, 2011, Open Access at Springerlink.com, DOI 10.1007/s00339-011-6264-9.

[5] Pershin, Y.V., Di Ventra, M. Experimental demonstration of associative memory with memristive neural networks. *Neural Networks*, vol. 23, no. 7, 2010, pp. 881-886.

[6] Chua, L.O. Nonlinear circuit foundations for nanodevices, Part I: The Four-Element Torus. *Proceedings of the IEEE*, vol. 91, no. 11, 2003, pp. 1830-1859.

[7] Chua, L.O., Szeto, E.W. High-Order Non-Linear Circuit Elements: Circuit-Theoretic Properties. *Int. J. of Circuit Theory and Applications*, vol. 11, 1983, pp. 187-206.

[8] Chua, L.O., Szeto, E.W. Synthesis of Higher Order Nonlinear Circuit Elements. *IEEE Trans. on Circ. Syst.*, vol. CAS-31, no. 2, February 1984, pp. 231-235.

[9] Benderli, S., Wey, T.A. On SPICE macromodelling of TiO2 memristors. Electronics Letters, vol. 45, no. 7, 2009, pp. 377–379.

[10] Biolek, D., Biolek, Z., Biolkova, V. SPICE Modeling of Memristive, Memcapacitative and Meminductive Systems. In *Proc. of ECCTD '09, European Conference on Circuit Theory and Design*, August 23-27, 2009, Antalya, Turkey, pp. 249-252.

[11] Biolek, Z., Biolek, D., Biolkova, V. SPICE model of memristor with nonlinear dopant drift. *Radioengineering*, vol. 18, no. 2, Part II, 2009, pp. 210-214.

[12] Biolek, D., Biolek, Z., Biolková, V. SPICE modelling of memcapacitor. *Electronics Letters,* vol. 46, no. 7, 2010, pp. 520 -522.

[13] Biolek, D., Biolek, Z., Biolková, V. PSPICE modeling of meminductor. *Analog Integrated Circuits and Signal Processing*, vol. 66, no. 1, 2011, pp. 129-137.

[14] Shin, S., Kim, K., Kang, S-M. Compact models for memristors based on charge-flux constitutive relationships. *IEEE Trans. Computer-Aided Design of Int. Circ. Syst*., vol. 29, no. 4, 2010, pp. 590–598.

[15] Biolek, D., Biolek, Z., Biolková, V. Behavioral Modeling of Memcapacitor. *Radioengineering*, vol. 20, no. 1, 2011, pp. 228-233.

[16] Biolek, D., Biolková, V., Kolka, Z. SPICE Modeling of Meminductor Based on its Constitutive Relation. In *Proc. of WSEAS Int. Conf. Instrumentation, Measurement, Circuits and Systems (IMCAS '11)*, Venice, Italy, 2011, pp. 76-79.

[17] Chua, L.O. Synthesis of New Nonlinear Networks Elements. *Proceedings of the IEEE*, vol. 56, no.8, 1968, pp. 1325-1342.

[18] Biolek, D., Bajer, J., Biolková, V., Kolka, Z. Mutators for Transforming Nonlinear Resistor Into Memristor. In *Proc. ECCTD 2011*, Linköping, Sweden, 2011, pp. 488-491.

[19] Biolek, D., Biolková, V., Kolka, Z. Mutators simulating memcapacitors and meminductors. In *Proc. APCCAS 2010*, Kuala Lumpur, Malaysia, 2010, pp. 800-803.

[20] Pershin, Y.V., Di Ventra, M. Memristive circuits simulate memcapacitors and meminductors. *Electronics Letters*, vol. 46, no. 7, 2010, pp. 517-518.

[21] Micro-Cap – Industrial Strength Simulation, http://www.spectrum-soft.com